Multicomponent Convection Induced by Fronts in the Chlorate–Sulfite Reaction

ARTICLE *in* THE JOURNAL OF PHYSICAL CHEMISTRY · FEBRUARY 1993

Impact Factor: 2.78 · DOI: 10.1021/j100115a058 · Source: NTRS

2 AUTHORS:

Istvan Nagy
University of Debrecen
33 PUBLICATIONS **597** CITATIONS
SEE PROFILE

John Pojman
Louisiana State University
238 PUBLICATIONS **4,139** CITATIONS
SEE PROFILE

Multicomponent Convection Induced by Fronts in the Chlorate–Sulfite Reaction

Istvan P. Nagy[†,‡] and John A. Pojman[*,†]

Department of Chemistry and Biochemistry, Box 5043, University of Southern Mississippi, Hattiesburg, Mississippi 39406, and Department of Physical Chemistry, Kossuth Lajos University, Debrecen, Hungary H-4010

Received: August 7, 1992; In Final Form: January 4, 1993

An application of a new method is presented for the measurement of the temperature profiles of chemical waves propagating through a solution. Using solutions of thermocolor materials, the temperature distribution caused by the heat released in the propagating chlorate oxidation of sulfite was visualized and recorded using digital image processing methods. After calibration, the temperature gradient was calculated from the gray scale value in a digitized image. Extensive multicomponent convection ("fingering") was induced by descending fronts. Only ascending fingers were observed because of the large thermal gradient that suppressed descending ones. The characteristics of the temperature profile were determined as a function of initial sulfite and chlorate concentration, and tube diameter. Unusual behavior was observed when the fronts propagated under conditions of continuously changing diameter in a conical vessel. Fingering occurred periodically in a front descending in a flask with an increasing diameter. However, when a front propagated down in flask whose diameter decreased, no multicomponent convection was observed.

Introduction

An autocatalytic reaction in an unstirred vessel can support a constant-velocity wave front resulting from the coupling of diffusion to the chemical reaction. Numerous reactions in solution have been described in which a front of chemical reactivity propagates through the medium from the site of an initial concentration perturbation.[1-13]

As a front propagates, concentration and thermal gradients are formed that alter the density of the solution, often causing convection.[6,13-20] Pojman and Epstein[21] have classified the types of convection that can occur in traveling fronts. If the reaction is exothermic ($\Delta H < 0$) and the products' solution is less dense than the reactants' ($\Delta V_{rxn} > 0$), then simple convection can occur, depending on the constraints of the container geometry. If the signs are the same, then simple convection will not occur. Instead multicomponent (double-diffusive) convection may occur, even though the overall density gradient may appear to be stable. In a descending front, double-diffusive convection manifests itself as "salt fingers", so-called because of their discovery in ocean layer mixing.

If a front of an exothermic reaction whose $\Delta V_{rxn} < 0$ (i.e., an isothermal density increase of the solution) propagates downward, then the system may appear to be stable to buoyancy-induced convection. In fact it is not. To understand how convection can occur, we must consider an analogous configuration with both salt and thermal gradients. We replace the product and reactant gradients by a single gradient of salt having the same density gradient as that induced isothermally by the traveling front and define a stability ratio:[22]

$$R_\rho = -\Delta\rho_T/\Delta\rho_c = -\Delta H^\circ/\beta C_p$$

where β is the mean molar isothermal density coefficient, $\partial\rho/\rho\partial C$. To simplify matters further, replace the smooth gradient occurring in the front by a sharp interface between solution layers. This approximation does not change the fundamental considerations.

Now consider hot, salty water above cold, fresh water as depicted in Figure 1. The system appears to be stable, if $R_\rho = 1$ (no net density gradient). Yet, it may not be. Imagine that

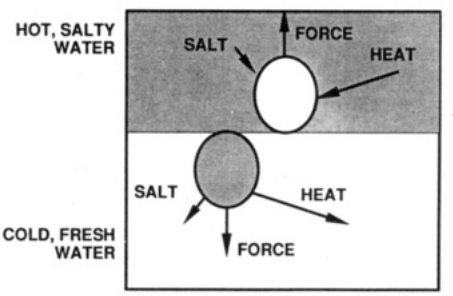

Figure 1. Mechanism for double-diffusive convection. $\Delta\rho_c$ and $\Delta\rho_T$ have opposite signs, and the net density gradient appears to be stable. However, if a small parcel of the warm, salty solution enters the lower section, because the heat diffuses faster than the salt, the parcel is left with a greater density than the surrounding medium, and it sinks. If a small parcel of cold, fresh water enters the warm, salty solution, heat will diffuse in faster than the salt. The parcel will be less dense than its surroundings and rise.

at the interface between the layers, a small parcel of the upper solution were to deviate from its position by gradually enlarging and descending into the cold, fresh region. Because the temperature and concentration are higher than in the surrounding region, heat and salt will diffuse out. The heat will leave at a greater rate, because of the larger diffusivity of heat (about two orders of magnitude). Now the parcel is cool and dense; because of its higher concentration, it sinks. Further, as the parcel contracts, the surface area to volume ratio increases, accelerating the loss of heat and the corresponding increase in density. Similarly, if a parcel of cold, fresh water protrudes into the hot, salty layer, heat will diffuse in faster than the salt. This will leave the parcel less dense than the surrounding layer, and the parcel will rise. What results are known as "salt fingers", which appear as long slender regions of alternately descending and ascending fluid.[22,23] This mechanism has been proposed to explain convective effects on chemical waves.[14,17,20,21]

The stability conditions for salt fingering have not been thoroughly studied for solutions in a narrow cylinder, although some preliminary work has been done.[24] Turner has shown that there is a critical value of R_ρ in an unbounded system.[22] The least stable configuration is a system with $R_\rho = 1$. If $R_\rho \gg 1$ for a reaction (i.e., very exothermic), Pojman and Epstein[21] predicted that it would be possible to suppress descending fingers under a downward propagating front.

[†] University of Southern Mississippi.
[‡] Kossuth Lajos University.

0022-3654/93/2097-3443$04.00/0

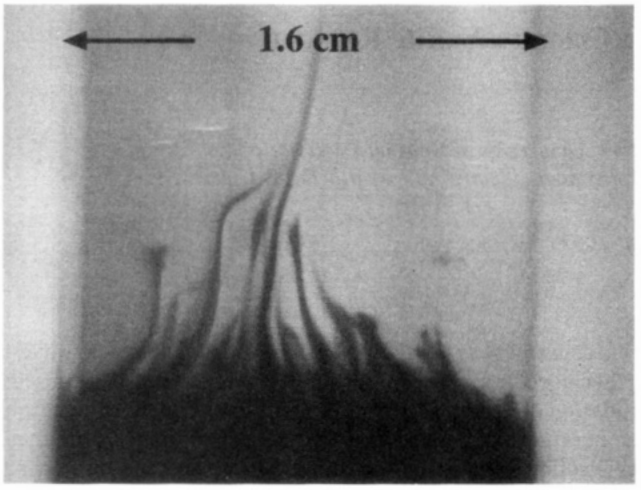

Figure 2. Multicomponent (double-diffusive) convection, also known as "fingering" is shown for a descending chlorate–sulfite front in a 2.2-cm i.d. tube with bromophenol blue as a pH indicator. Initial concentrations: $[KClO_3]_0 = 0.325$ M; $[Na_2SO_3]_0 = 0.832$ M; $[H_2SO_4]_0 = 0.115$ M.

To understand the chemical mechanism and the role of convection in front propagation, it is important to measure the concentration and thermal gradients. The use of digital image processing is a powerful technique for the measurement of concentration gradients.[25]

The standard method to measure the temperature distribution is to use a series of thermocouples or thermoelements.[15,17] The resolution is limited by the minimal size of the measuring devices and manipulating a large number of such devices is cumbersome.

Another possible solution is to use infrared imaging, but the cost of an instrument with the necessary resolution and temporal response is very high, being orders of magnitudes higher than the price of a standard image-processing system.

We can combine temperature measurements with image processing by making the temperature distribution visible using thermocolor compounds. If the color change related to the temperature change has sufficient contrast, it can be captured by a camera and analyzed using image-analysis software.[26]

To test predictions on fingering, we have studied the chlorate oxidation of sulfite[27,28] because it is a very exothermic reaction ($\Delta H = -845$ kJ/mol)[29] whose $\Delta V_{rxn} < 0$, and the progress of the front can be seen with a pH indicator:[30]

$$ClO_3^- + 3HSO_3^- \rightarrow Cl^- + 3HSO_4^-$$

The oxidation of bisulfite to bisulfate is weakly autocatalytic. The oxidation is believed to occur via the oxidation of H_2SO_3, formed from the protonation of bisulfite.[27,28] Conversion of the weak acid bisulfite ($K_a = 6.2 \times 10^{-8}$) to the stronger acid bisulfate ($K_a = 0.010$)[29] results in a net release of H^+, which protonates more bisulfite.

In the preliminary experiments carried out in vertical tube (1.6-cm i.d.), a highly exothermic chemical wave was observed after the front was initiated at the top of the tube with a few drops of 3.0 M sulfuric acid. Significant multicomponent convection occurs as shown in the Figure 2, where the lighter upper section is the reacted solution having a yellow color indicating a low pH; the dark region is the unreacted, basic solution. If fronts propagate through a solution filled with ultrafine silica gel, they propagate extremely slowly (≈2 cm/h). The silica gel not only prevents convection, but also reduces the amount of heat generated per volume; thus an isothermal front propagates. In tubes of 1.5-cm i.d. and larger without silica gel, fronts propagate on the order of 1 cm/min. It is not clear how much of this increase is caused by convection and how much is caused by the increase of the temperature.

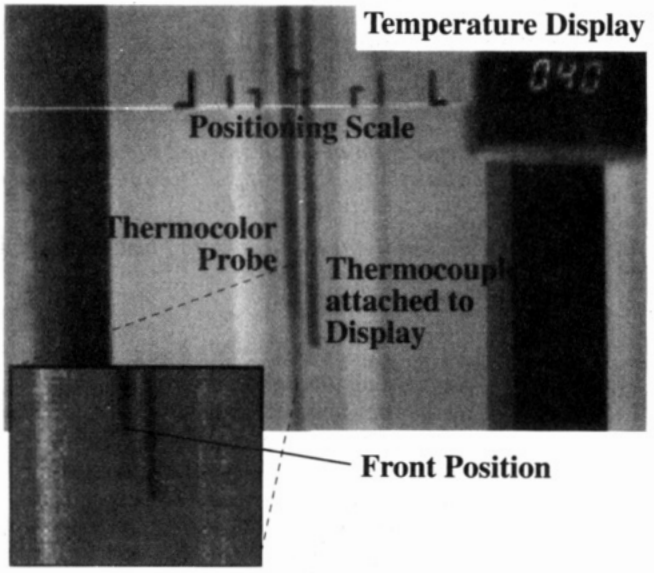

Figure 3. Frame of interest in the subject plane of the device used to study one-dimensional temperature distributions. The inset shows the gray scale gradient as it appears in the position of the front. Notice that the reaction mixture is itself colorless, and the illumination was chosen to suppress the contrast between the test tube and the surroundings.

Experimental Section

To monitor the temperature profile of a descending front in a vertical reaction vessel, we used a custom-built apparatus and a method visualizing and measuring heat gradients using a thermocolor solution.[26] A thermocouple is used to measure the temperature at one point of the thermocolor probe as a confirmation of the temperature calculated from the calibration curve. Images from an Hitachi KP-C501 solid state color camera equipped with a Cosmicar zoom lens were digitized with a RasterOps 364 board on a Macintosh Quadra 700 and saved as PICT files. Analysis of captured images was performed with Image Analyst v. 7.22 (Automatrix, Inc.).

The thermocolor mixture used in the 20–90 °C temperature range was prepared by mixing two stock solutions. One was an aqueous solution of 0.34 g of $Co(Cl_2)\cdot 6H_2O$, 0.02 g of $CuSO_4\cdot 5H_2O$, 0.02 g of KBr, and 0.06 g of NaCl dissolved in 1 mL of water. The other stock solution contained ethanol, *n*-hexanol, acetone, and acetic acid in 3:1:1:1 volume ratio. The two stock solutions were mixed immediately before use in a 1:6 (aqueous to organic) ratio. It is important to note that before use the mixture should be heated to boiling in a closed vessel to dissolve any solid salt remaining in the bottom of the solution. The solution is over saturated and material can precipitate; it was prepared fresh for each experiment. Capillary tubes were filled with the mixture and sealed before using.

To yield a calibration curve we filled a 1.4-cm i.d. tube with boiling water and let it cool down slowly. Pictures were collected for each 2–3 °C decrease in temperature down to room temperature. The gray scale distribution of the part of the picture containing the thermocolor probe (Figure 3) was checked using a histogram showing the population of the pixels with several gray scale values as a function of the absolute gray scale range. A column of pixels in the picture of the thermocolor probe was chosen and written to a data file. The average of each data set was taken, and the temperature–gray scale calibration curve shown in Figure 4a was calculated.

To determine thermal front profiles, a particular column of the region of the picture containing the image of the thermocolor probe was written to a data file including coordinates of the pixels and the gray level values. The gray scale values were transformed into temperature values. A gray scale distribution as a function of the geometric position and the corresponding temperature distribution are shown in Figure 4b,c, respectively.

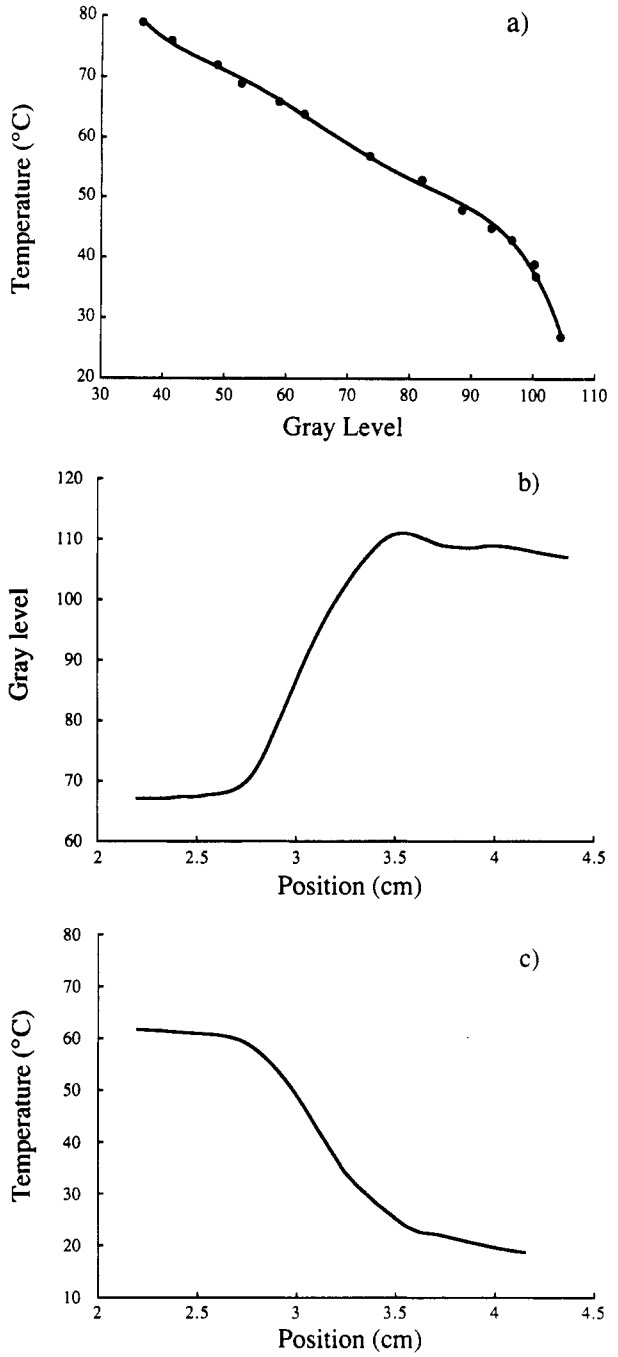

Figure 4. (a) Gray scale vs temperature calibration curve used to determine thermal profiles. (b) Particular gray scale distribution in the direction of the wave propagation. (c) Thermal profile determined with the combination of the gray scale distribution and the calibration function in Figure 4a.

The accuracy of the method was checked with several parallel experiments, refilling the test tube containing the thermocolor probe and a thermocouple shown in Figure 3 with water having a known temperature. The analysis of the pictures processed showed that the temperature resolution of the method under the conditions discussed is 0.5 °C in the region of 44–90 °C, which is limited by inhomogeneities in the illumination and noise arising from the so-called neighborhood effect of the CCD elements of the camera. In the range 25–44 °C the sensitivity and the reproducibility are only 1.5–2.5 °C, limited by the CCD matrix characteristics and the gain-offset capabilities of the camera.

Mixtures for the wave experiments were prepared by dissolving the necessary amounts of potassium chlorate and sodium sulfite, then acidifying with 2.30 M sulfuric acid stock solution. About 2 mg of bromophenol blue was added as indicator if it was necessary to see the front.

To minimize the mixing effect arising from the density difference of the reaction mixture and the initiating acid solution, a filter paper ring was immersed partly under the top of the solution and was carefully impregnated with the acid solution. In this way the wave was initiated in a reproducible way.

The change in density of the reaction solution was determined by measuring the densities of the initial and final solutions with a pycnometer.

Results

We studied the temperature profiles of descending waves as a function of the $[KClO_3]_0$. After obtaining a profile such as shown in Figure 4c, we determined the temperature difference between the reacted and unreacted sides of the front. We evaluated the value (°C/cm) of the gradient by determining the slope of the linear function fitted on the inflection point of the gradient. The width of the front was taken as the distance between the intercept points of the slope and the lines indicating the minimal and maximal temperatures between the two sides of the front.

Results show that an increase in the chlorate concentration increases the temperature difference, but after a certain concentration it levels off at a constant value of about 40 °C (Figure 5a). The front width (Figure 5b) has a maximum at approximately 0.28 M $[KClO_3]_0$ where the front is the most diffuse in spite of the relatively large temperature difference. The slope of the gradient shows a monotonous increase as a function of the initial chlorate concentration (Figure 5c).

The $[Na_2SO_3]_0$ dependence of the front width shows a monotonically increasing temperature difference (Figure 6a), which indicates that the heat released is related to the amount of the sulfite consumed during the reaction. (Higher sulfite concentrations were precluded by solubility.) The maximum ΔT = 45 °C is less than the 60 °C expected from the ΔH of reaction. This may be due to convective heat losses or because the reaction does not strictly follow the proposed stoichiometry. Figure 6b shows the front width decreasing with increasing sulfite but the thermal gradient roughly increases linearly.

The temperature difference exhibits a maximum as a function of tube diameter (Figure 7a) caused by the competition between heat loss to the environment and convective transport. The surface area to volume ratio decreases with increasing tube diameter, and so the heat loss decreases as the temperature difference increases. However, the amount of convection also increases with tube diameter, and this convective transport reduces the temperature difference. Figure 7b shows that the front width decreases and the overall thermal gradient (Figure 7c) increases with diameter.

To gain a more detailed understanding of the diameter dependence of the convective phenomena, we used a separatory funnel, inverted with the stopcock on top, and initiated the front so that it would be propagating down and into regions with progressively larger diameters. We expected that the fingering would increase monotonically or that a critical diameter would be found. Instead, we observed a periodic appearance and disappearance of the fingering as the wave propagated (Figure 8a). Fingering was observed initially (Figure 8a-1), disappeared (Figure 8a-3), reappeared (Figure 8a-4), disappeared, and then reappeared (Figure 8a-7). The total suppression of the fingering is observed in two regions, shown on Figure 8a-3 and a-6.

Both the appearance and disappearance of the fingering are coupled to a formation of an axisymmetric region of fingering, as is shown in Figure 8a-7. The last region of fingering to disappear was in the center. Fluid motion was observed to occur axisymmetically, with fluid flowing in toward the center, rising and circling back down the walls of the funnel. When fingering

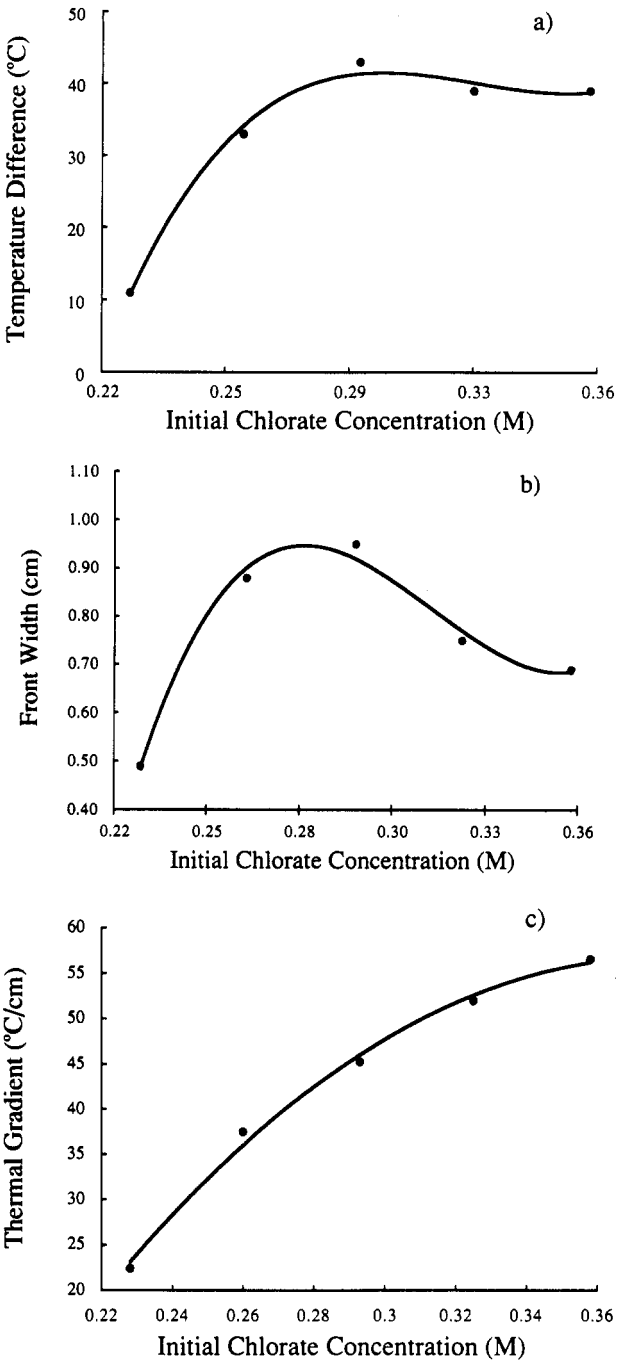

Figure 5. Parameters evaluated from thermal profiles to describe $[KClO_3]_0$ dependence of the convective phenomena (see Figure 2). (a) Temperature difference between the reacted and unreacted sides of the reaction front. (b) Front width as a function of the $[KClO_3]_0$. (c) The thermal gradient evaluated using data of Figure 4a,b. Initial concentrations in all cases: $[Na_2SO_3]_0 = 0.832$ M; $[H_2SO_4]_0 = 0.115$ M; tube diameter (internal) = 1.4 cm.

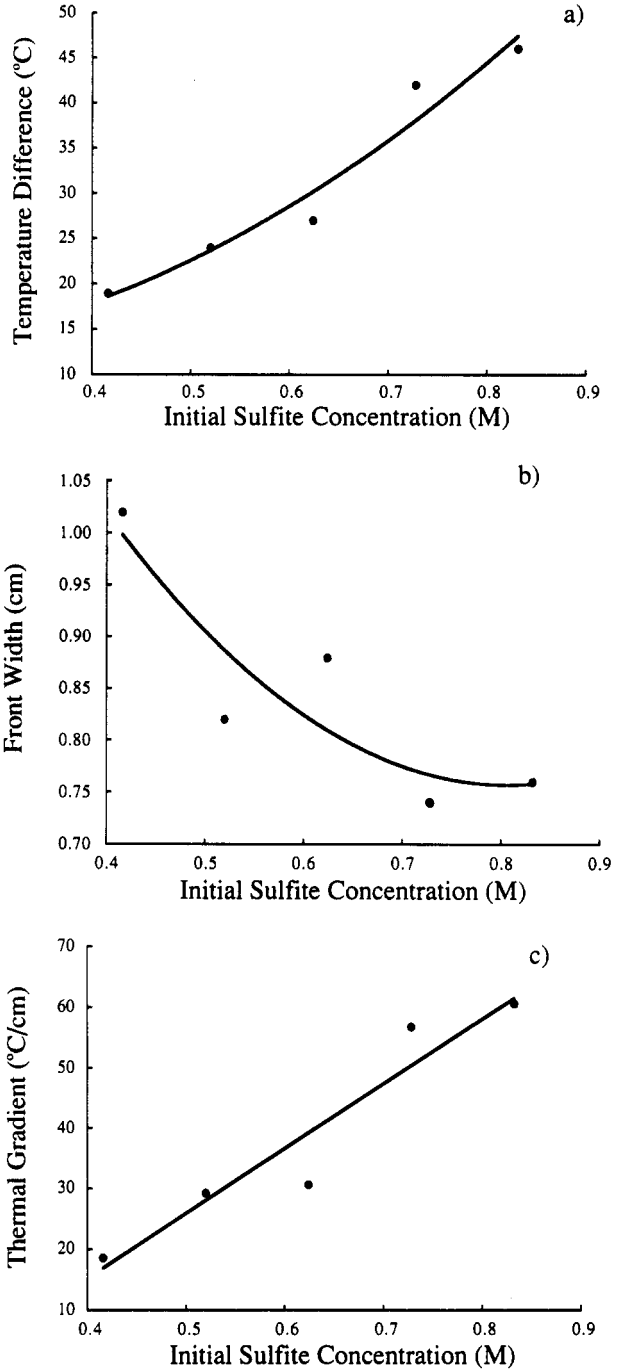

Figure 6. Parameters evaluated from thermal profiles to describe $[Na_2SO_3]_0$ dependence of the convective phenomena (see Figure 2). (a) Temperature difference between the reacted and unreacted sides of the reaction front. (b) Front width as a function of the tube diameter. (c) The thermal gradient evaluated using data of Figure 6a,b. Initial concentrations in all cases: $[KClO_3]_0 = 0.325$ M; $[H_2SO_4]_0 = 0.115$ M; tube diameter = 1.4 cm.

reappeared, a small amount of fingering was observed in the center, and the fingering spread out until a uniform zone was formed.

We carried out an experiment using the same concentrations, initiating a descending wave in an inverted separatory funnel. As it is shown on the Figure 8b-2–8b-6, fingering never extended across the whole cross section of the front, nor were there any stages of the total fingering suppression. Fronts with the same concentrations were observed in constant diameter tubes whose diameters equaled the critical diameters when fingering appeared and disappeared. In these cases, as it is shown Figure 8c-1–8c-6, stable fingering zones were observed across the entire cross section of the tube.

In the case when the periodic fingering was observed, we carried out temperature measurements to study the vertical temperature distribution in the geometric center of the funnel. The experimental method and apparatus were close to the those described in the experimental section, but because the different geometry of the frame of interest we had to change the illumination. That is the reason the calibration function is not the same as shown on the Figure 4a. An additional problem was also the decreased sensitivity because we could not use an intensive light source without distorting the uniformity of the illumination of the frame of interest shown in Figure 9a.

The thermal profiles shown in Figure 9b-1–b-8 support the observation of the periodic fingering, because a periodic change

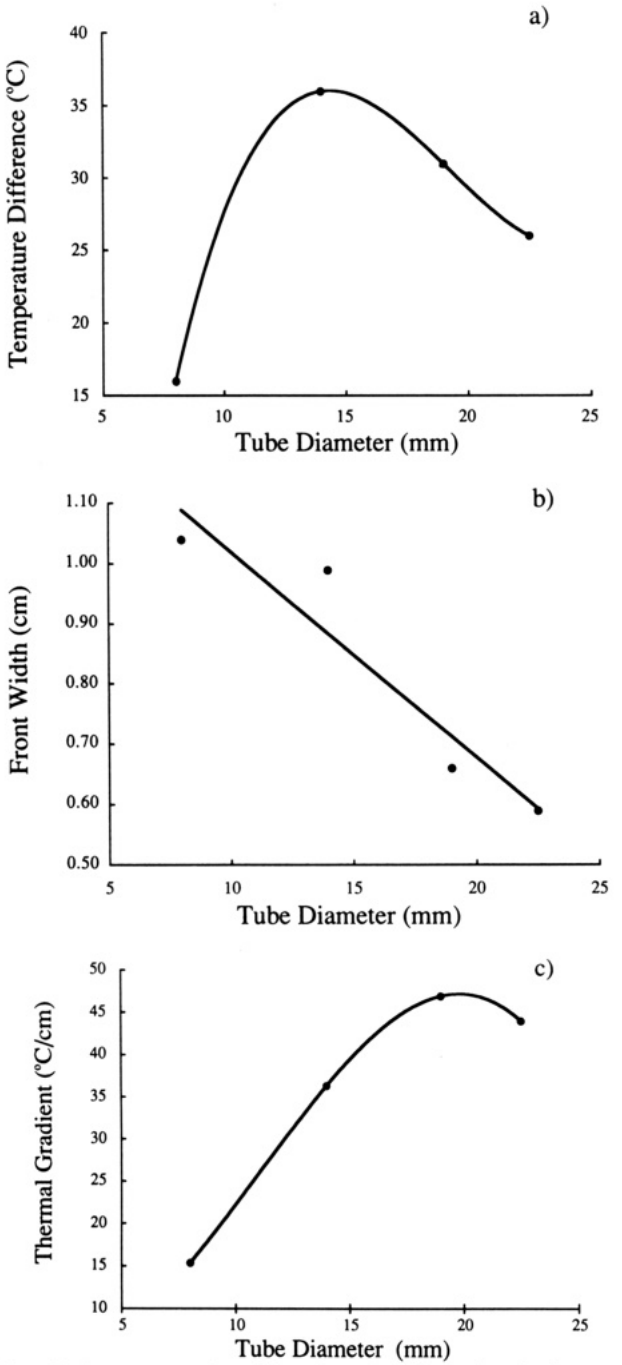

Figure 7. Parameters evaluated from thermal profiles to describe diameter dependence of the convective phenomena (see Figure 2). (a) Temperature difference between the reacted and unreacted sides of the reaction front. (b) Front width as a function of the tube diameter. (c) Thermal gradient evaluated using data of Figure 7a,b. Initial concentrations in all cases: $[KClO_3]_0 = 0.325$ M; $[Na_2SO_3]_0 = 0.832$ M; $[H_2SO_4]_0 = 0.115$ M.

in a thermal profile can be also observed. Figure 9b-2 shows a definitely sharper front than Figure 9b-1 and 9b-3. The profiles in 9b-1 and 9b-3 belong to a fingering stage, having a more diffuse thermal profile than Figure 9b-2 in which fingering was suppressed. Figure 9b-5 corresponds to a flat front having a sharper boundary than the next and previous stage showing the more diffuse, broader profile of fingering.

Experiments also were carried out in a Petri dish to find two-dimensional structures caused by convection, which are similar to those reported for other systems.[20,31] In a 0.5–1.5-cm layer we observed several kinds of structures (Figure 10a,b) that depend on the thickness of the liquid poured into the vessel.

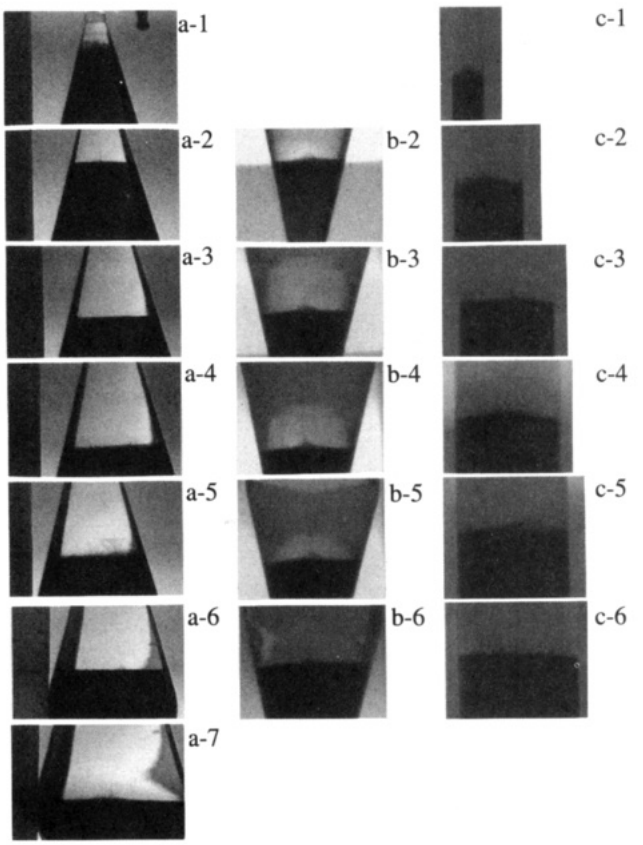

Figure 8. Periodic fingering and convective hysteresis in the chlorate–sulfite reaction. Same conditions as Figure 2.

Discussion

The isothermal density change for a reaction consisting of 0.83 M $[Na_2SO_3]_0$, 0.12 M $[H_2SO_4]_0$, and 0.33 M $[KClO_3]_0$ was $+5.4 \times 10^{-3}$ g/cm^3 (0.48 %), a large value compared to changes in other systems for which multicomponent convection has been proposed.[14,20] The isothermal density increase means a $\Delta V_{rxn} < 0$, which is consistent with the appearance of "salt fingers" shown in Figure 2. Although multicomponent convection had been proposed to explain convective effects in the iron(II)–nitric acid system, fingering was never directly observed.[14] Thus, the analysis of Pojman and Epstein is further supported.

Let us repeat our stability for the fluid with temperature and concentration gradients created by a descending wave front. Suppose a warm parcel of the reacted solution (above the wave front) enters the lower region by moving a distance δz. The time required for enough heat to diffuse out until the density of the parcel is greater than the unreacted solution is τ. If the reaction-diffusion wave front velocity is v, then the time until the parcel is surrounded by solution of the same composition is $\delta z/v$. If $\tau > \delta z/v$, then no fingers can form. If $R_\rho > 1$, then the descending fingers may be suppressed while the ascending ones still occur. To see why this can be, consider that the descending fingers may not occur because the front "catches up" with the finger before it can completely form. However, the ascending finger can proceed and will be assisted by conversion of solution around it to the hot, reacted solution. This can be seen in Figure 2.

For the case of simple convection, it is known that there are critical values of the Raleigh number (itself of function of tube diameter) at which various modes of convection arise.[15,21] Less is known about the behavior of multicomponent convection although below a critical diameter, no convection occurs.[6,14,20] The behavior shown in Figure 8a would seem to indicate that there are critical diameters at which double-diffusive convection can occur. (The diameters are much larger than in any previous front experiments.) The behavior shown in Figure 8b,c indicates

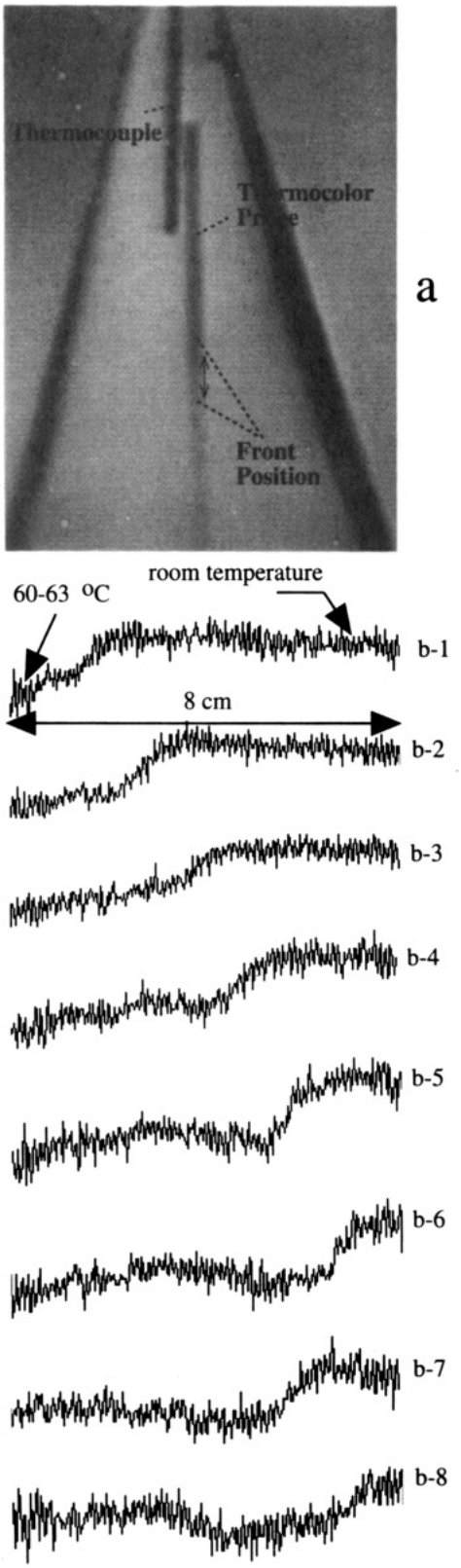

Figure 9. Temperature profile measurement on the periodic fingering phenomena using thermocolor probe. (a) Frame of interest. (b) Qualitative thermal profiles indicating different stages of the periodic hydrodynamic phenomena. Initial concentrations: $[KClO_3]_0 = 0.325$ M; $[Na_2SO_3]_0 = 0.832$ M; $[H_2SO_4]_0 = 0.115$ M.

the system is more complicated. The images in Figure 8c are from experiments performed in tubes with the same diameters of the funnel at the front position in Figure 8a. Convection occurs in all tubes, irrespective of the diameter. Thus, the stability condition for convection is not a simple function of the diameter.

Further support for this analysis comes from the experiments

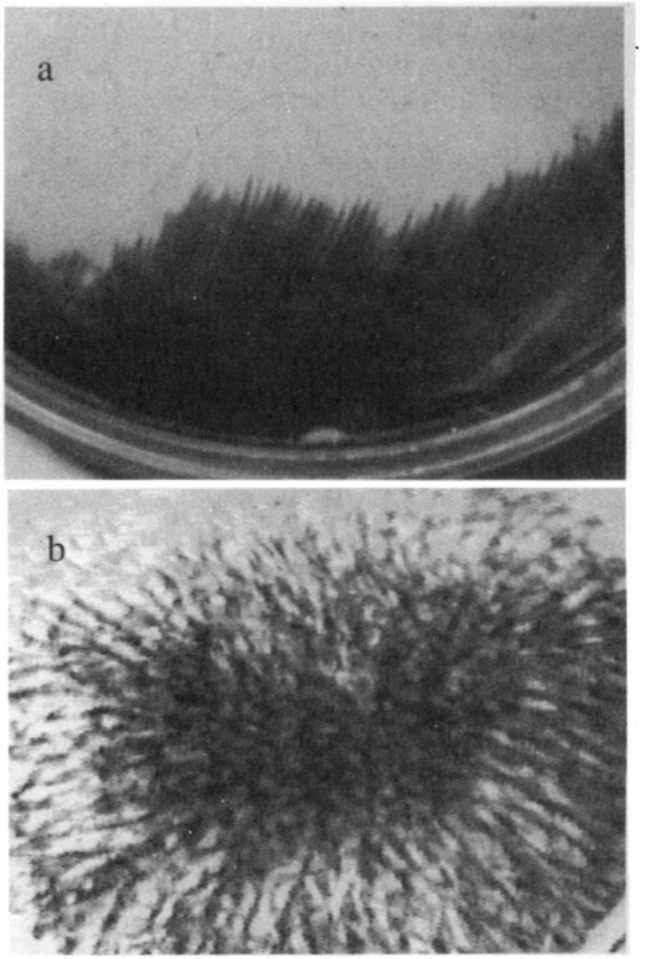

Figure 10. Two-dimensional phenomena in a Petri dish filled with the reaction mixture: (a) 0.5-cm; (b) 1.5-cm layer of solution. Initial concentrations: $[KClO_3]_0 = 0.325$ M; $[Na_2SO_3]_0 = 0.832$ M; $[H_2SO_4]_0 = 0.115$ M.

in which the separatory funnel was inverted. As shown in Figure 8b, fingering occurred at diameters when fingering did not occur with the tube in the reverse orientation (compare Figure 8a-3 and b-3). The origin of this behavior must result from the nature of the container above the front. In Figure 8b, the fingering occurred axisymmetrically around a central zone and never completely across the front, which suggests that an expanding volume above the front more readily accommodates large scale fluid motion than a contracting volume. The funnel shape allows hot fluid at the front to rise and expand, descending along the walls as it cools. This pattern must not occur as readily in a container with a uniform (or decreasing) diameter.

Although the thermal gradient decreases when there is no fingering (Figure 9b-3), it is not clear if this is the cause of, or a result of, the lack of fingering. We do not have an explanation but suggest that a full computational model will need to be developed before an adequate explanation for these phenomena can be offered.

Conclusion

We applied thermocolor imaging to fronts of the chlorate–sulfite reaction and measured thermal gradients as a function of initial reactant concentrations and tube diameter. Results indicate that sulfite is the limiting reagent. The tube diameter affects the gradient by altering the surface area to volume ratio and by changing the ability of the system to support convection.

We have confirmed that $\Delta V_{rxn} < 0$, providing additional support for previous explanations of multicomponent convection induced by traveling fronts. We have also demonstrated that descending convective fingering can be suppressed, as predicted.

The appearance of multicomponent convection is not a simple function of tube diameter in a conical vessel. The fingering can appear then disappear and then appear as the front descends in a funnel whose diameter increases along the direction of propagation. Such periodicity does not occur if the funnel orientation is reversed.

Acknowledgment is made to the donors of the Petroleum Research Fund, administered by the ACS for partial support of this research. We also acknowledge support from the National Science Foundation's Mississippi EPSCoR Program and from NASA's Microgravity Materials Science Program. Istvan P. Nagy thanks the OMFB (National Board for the Technical Development in Hungary) for travel support.

References and Notes

(1) Zaikin, A. N.; Zhabotinskii, A. M. *Nature* **1970**, *225*, 535–537.
(2) Winfree, A. T. *Science* **1973**, *181*, 937–939.
(3) Field, R. J.; Noyes, R. M. *J. Am. Chem. Soc.* **1974**, *96*, 2001–2006.
(4) Reusser, E. J.; Field, R. J. *J. Am. Chem. Soc.* **1979**, *101*, 1063–1071.
(5) Gribshaw, T. A.; Showalter, K.; Banville, D. L.; Epstein, I. R. *J. Phys. Chem.* **1981**, *85*, 2152–2155.
(6) Bazsa, G.; Epstein, I. R. *J. Phys. Chem.* **1985**, *89*, 3050–3053.
(7) Hanna, A.; Saul, A.; Showalter, K. *J. Am. Chem. Soc.* **1982**, *104*, 3838–3844.
(8) Field, R. J.; Burger, M. *Oscillations and Traveling Waves in Chemical Systems*; Wiley: New York, 1985.
(9) Harrison, J.; Showalter, K. *J. Phys. Chem.* **1986**, *90*, 225–226.
(10) Szirovicza, L.; Nagypál, I.; Boga, E. *J. Am. Chem. Soc.* **1989**, *111*, 2842–2845.
(11) Ross, J.; Müller, S. C.; Vidal, C. *Science* **1988**, *240*, 460–465.
(12) Pojman, J. A. *J. Am. Chem. Soc.* **1991**, *113*, 6284–6286.
(13) Tzalmona, A.; Armstrong, R. L.; Menzinger, M.; Cross, A.; Lemaire, C. *Chem. Phys. Lett.* **1992**, *188*, 457–461.
(14) Pojman, J. A.; Epstein, I. R.; Nagy, I. *J. Phys. Chem.* **1991**, *95*, 1306–1311.
(15) Pojman, J. A.; Epstein, I. R.; McManus, T.; Showalter, K. *J. Phys. Chem.* **1991**, *95*, 1299–1306.
(16) Vasquez, D. A.; Edwards, B. F.; Wilder, J. W. *Phys. Rev. A.* **1991**, *43*, 6694–6699.
(17) Pojman, J. A.; Craven, R.; Khan, A.; West, W. *J. Phys. Chem.* **1992**, *96*, 7466–7472.
(18) Miike, H.; Muller, S. C.; Hess, B. Interaction of Chemical Waves and Hydrodynamics Flow; In *Cooperative Dynamics in Physical Systems*; 1989; pp 328–329.
(19) Miike, H.; Müller, S. C.; Hess, B. *Chem. Phys. Lett.* **1988**, *144*, 515–0520.
(20) Nagypál, I.; Bazsa, G.; Epstein, I. R. *J. Am. Chem. Soc.* **1986**, *108*, 3635–3640.
(21) Pojman, J. A.; Epstein, I. R. *J. Phys. Chem.* **1990**, *94*, 4966–4972.
(22) Turner, J. S. *Buoyancy Effects in Fluids*; Cambridge University Press: Cambridge, 1973.
(23) Turner, J. S. *Annu. Rev. Fluid Mech.* **1985**, *7*, 11–44.
(24) Georgopolous, E.; Horwitz, J. A. *Acta Mech.* **1987**, *70*, 177.
(25) Nagy, I.; Póta, G.; Bazsa, G. *J. Chem. Soc., Faraday Trans.* **1991**, *87*, 3613–3615.
(26) Nagy, I. P.; Pojman, J. A. *Chem. Phys. Lett.* **1992**, *200*, 147–152.
(27) Halperin, J.; Taube, H. *J. Am. Chem. Soc.* **1960**, *72*, 3319–3320.
(28) Halperin, J.; Taube, H. *J. Am. Chem. Soc.* **1952**, *74*, 375–380.
(29) Dean, J. H. *Lange's Handbook of Chemistry*; McGraw-Hill: New York, 1985.
(30) Summerlin, L. R.; Borgford, C. L.; Ealy, J. B. *Chemical Demonstrations*; American Chemical Society: 1988.
(31) Orbán, M. *J. Am. Chem. Soc.* **1980**, *102*, 4311–4314.